CALCULATION OF THE EFFECTS OF A CARGO FIRE IN A HOLD OF A SHIP

J. K. Cole, J. A. Koski, and S. D. Wix

Sandia National Laboratories*, P.O. Box 5800, Albuquerque, NM 87185-0717

INTRODUCTION

To better understand shipboard fire environments, a combined experimental and computational study has been conducted at Sandia National Laboratories to define problems that could develop and to demonstrate that modern computational fluid dynamics (CFD) tools can adequately model fires in enclosed volumes (e.g., the holds of ships). A simulated shipping cask was used as a test object (calorimeter) in this study.

Fuel and wood fire experiments were staged by the Coast Guard in Hold 4 of the *Mayo Lykes*, a 10,700 deadweight ton, World War II, Liberty Class, freighter located in Mobile Bay, Alabama, USA in 1995. During these tests, temperatures and heating rates were measured in Holds 4 and 5.

This paper describes the development of a computational model for a wood crib fire located in the same hold as the test object. The commercially available CFD code used was CFX, developed by Harwell Laboratory, United Kingdom. This finite volume code was selected because of its previous use in fire analyses and its ability to treat all heat-transfer mechanisms (i.e., conduction, convection, and thermal radiation) in a coupled manner. Comparisons are made between experimental measurements and blind computational results, i.e., no experimental data were used to make the computations.

HOLD MODEL DESCRIPTION

Hold Model - Hold 4 of the *Mayo Lykes* is located one level below the weather deck. The arrangement of the hold is symmetrical with respect to the ship's longitudinal axis. During the fire tests, this symmetry was maintained by positioning the centerlines of the fire and the simulated shipping cask (calorimeter) on the ship's centerline. In the modeling, it was assumed that the thermal/flow processes maintained this symmetry.

---

* Sandia is a multiprogram laboratory operated by Sandia Corporation, a Lockheed Martin Company for the United States Department of Energy under Contract No. DE-AC04-94AL85000.

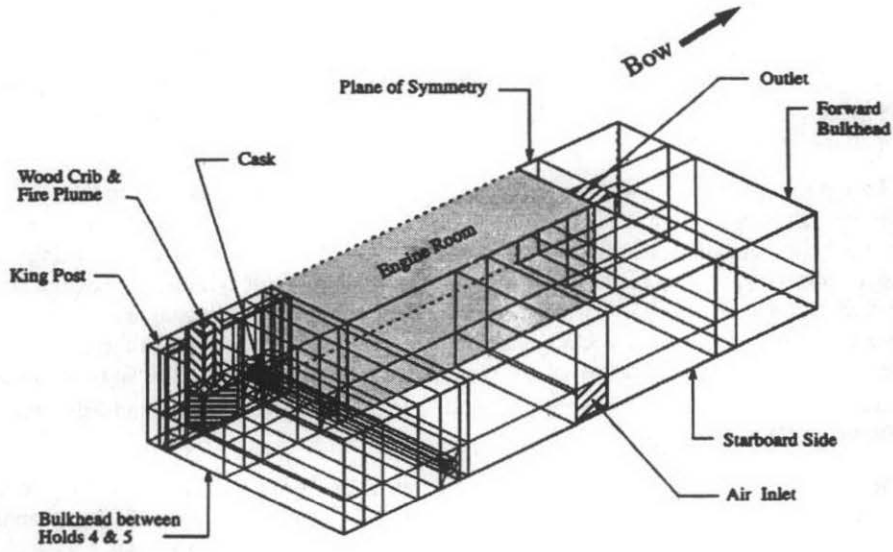

Figure 1. Hold 4 of the *Mayo Lykes*.

Figure 1 shows the starboard (right) half of Hold 4 which was modeled in the CFX code. The overall dimensions of this half were 21.2 m long x 8.9 m wide x 3.7 m tall.

An expanded view of the region of Hold 4 in which the fire is located is shown in Figure 2.The bulkheads (walls) were 0.008 m thick, the deck and overhead, 0.011 m thick and the hull, 0.018 m thick. These were all treated as conducting solids, made of mild steel with a density of 7837 kg/m,^{3} a specific heat of 460 J/(kg K), and a thermal conductivity of 45 W/(m-K).

The outer surfaces of all of the bulkheads, deck, and overhead that define the extent of Hold 4 were subjected to convective and radiative heat transfer assuming a constant atmospheric temperature of 303 K. The radiative emissivity was 0.8 for these outer surfaces. The convective heat transfer coefficient was varied depending upon the orientation of each surface. The values

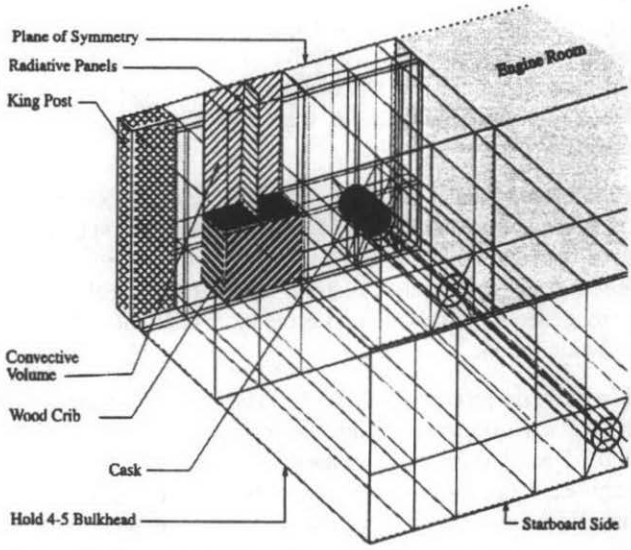

Figure 2. Expanded view of wood crib and calorimeter.

used for the bulkheads and hull, lower surface of deck, and upper surface of overhead, were 1.58, 1.05, and 2.00 W/(m^2 K), respectively.

Shear stresses on the inner surfaces of the bulkheads, deck and overhead were not specified so that CFX could force the fluid velocity to zero at each of these surfaces. On the plane of symmetry, the shear stresses were set to zero to prevent the generation of a boundary layer.

A king post (mast) intersected the bulkhead separating Hold 4 from Hold 5 so that approximately half of it extended into each hold. The portion in Hold 4 was reinforced with large trapezoidal steel plates welded to both sides of the king post. The resulting shape approximated a rectangular object more closely than a half cylinder. The actual king post was hollow, but to simplify the CFX model, the king post in the simulation was assumed to be a conducting, rectangular solid. To give the model king post the same thermal mass and thermal diffusivity as the real one, its thermal properties were modified to a density of 520 kg/m^3, a specific heat of 460 J/(kg K), and a thermal conductivity of 3.06 W/(m K).

Calorimeter (Cask) Model - The calorimeter was made from a mild steel cylinder with a wall thickness of 0.025 m, an outside diameter of 0.61 m and a length of 1.83 m. Its ends were covered by steel disks, 0.025 m thick and its interior filled with 128 kg/m^3 Kaowool insulation. In the CFX simulation, the right half of this calorimeter was modeled as a steel cylinder of the proper dimensions with an insulated interior. An end cover was not included in the model since it has little influence on the temperatures of the steel cylinder in this side-on orientation to the fire.

Modeling of Openings - In both halves of Hold 4, there were one opening (Inlet) near deck level and one (Outlet) near the top of the forward bulkhead of the engine room. The lower edge of the entrance penetrated the hull about 0.5 m below the deck and several steps were required to reach deck level. The indentation in the deck created by the enclosed stairwell was not modeled. Instead the CFX model used an opening whose upper edge was located at the same height above the deck as that of the actual entrance and whose lower edge was at deck level. To provide the same flow area as the actual entrance, the model entrance was made wider. This 1.30 m tall x 1.41 m wide entrance was centered longitudinally in the hold. For the wood crib fire tests, the Outlet in the overhead was closed.

Radiation Model - The CFX code offers two methods for calculating the radiative heat transfer between surfaces, a Monte Carlo simulation and a discrete transfer method developed by Shah. See Guilbert 1989. This problem had a fixed, rather simple geometry and assumed gray body radiation. The radiation field was expected to be reasonably homogeneous. Shah's method is the more efficient under tnese conditions and was used in this simulation.

The radiative properties for the various surfaces in the hold were emissivity and roughness of: 0.8 and 1.0 for the bulkheads, deck and overhead, 0.9 and 1.0 for the plume and crib, and 1.0 and 0.0 for the symmetric surface, respectively. Note that as the roughness parameter for a surface is increased from 0.0 to 1.0, its spectral reflection decreases linearly from 100 to 0 percent and its diffuse reflection increases linearly from 0 to 100 percent.

Wood Crib Fire Model - The actual combustion processes in burning a wood crib were not modeled. Instead, the measured thermal energy released over time in burning a standard wood crib was used. This model included both radiative and convective parts, see Figure 3. The radiative parts were the lateral and top faces of the wood crib, the plume wall radiator in the plane of symmetry and the plume center radiator that extended from the top of the crib to the overhead. The convective part was the air volume between the top of the wood crib and the overhead. The crib was assumed to maintain its original shape for the entire burn.

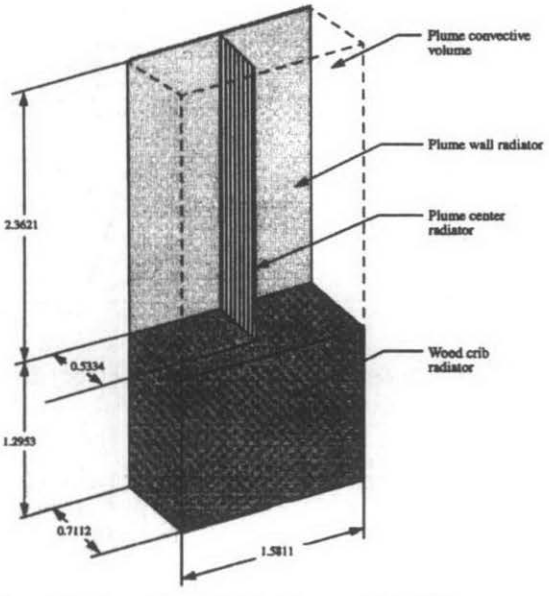

Figure 3. Thermal model for the wood crib fire.

The actual wood crib was constructed of nominal 0.05 x 0.10 m (2 x 4 inches), Douglas fir boards, 1.52 m (62.25 inches) long. These were placed in alternating layers with the lengths of the boards in each layer being at right angles to those in the adjacent layers. This wood was assumed to reach a steady burn 30 seconds after ignition and to burn at a constant rate for 1170 seconds. After that the crib burned out in 300 seconds. A pool of heptane accelerant was used at the beginning of the wood fire. It was also assumed to reach a steady burn within 30 seconds, to burn steadily for 270 seconds. and then burn out within 30 seconds. The maximum rate of thermal energy released by the wood and the accelerant during the first 300 seconds of the burn was calculated to be 2.37 mW and 1.73 mW, respectively. These values for the whole fire were halved for the simulation of the starboard half of the hold.

In the fire model, the crib was assumed to contribute substantially in releasing energy as a radiant heat source. The calculated maximum heat released from the wood crib and the heptane accelerant during the first 300 seconds of the burn was divided about equally between convective and radiant heat transfer. The radiant heat release of the wood crib was then held at this same level until burnout commenced at 1200 seconds. The outer surfaces of the wood crib was assigned an emissivity of 0.5 and the plume surfaces, 0.9. During the steady burn, the crib radiated at 56.9 kW/m^2 and the plume surfaces at 102.3 kW/m^2.

The surfaces of the plume wall radiator and the plume center radiator were assigned zero shear stresses so no boundary layers developed on them. Flow was not permitted to pass through these surfaces.

The large transient due to the heptane accelerant was assigned almost entirely to the

convective heat release. The convective energy was deposited directly into the air volume between the top of the crib and the overhead. This energy deposition decreased from about 354 to 66 kW/m^3 as the accelerant burned out at 300 seconds. Figure 4 shows the heat flux versus time for the total energy released as well as the energy partitioning between radiation and convection that was used in the model. All of the transients in energy release were modeled with cosine functions.

Simulation of Smoke Effects - In the fire experiments, considerable smoke was generated. To approximate the decreased transparency of the air due to this smoke, the absorptivity of the air was made a function of air temperature. *The Handbook of Geophysics and Space Environment*, 1985, indicates that clear air has an absorptivity around 6 x 10^{-5} m^{-1} and light fog, around 6 x 10^{-3} m^{-1}. The smoke was assumed to be associated with the hotter air, which allowed an S-shaped function to be defined to vary the air absorptivity between zero absorptivity at 300 K and an absorptivity of 10 m^{-1}at 1200 K in approximate agreement with the geophysical data. Fire solutions were calculated with this smoke model and also with a transparent air model which had a gas absorptivity of 1 x 10^{-3} m^{-1}.

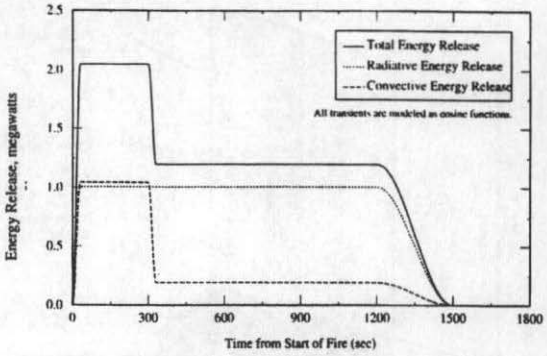

Figure 4. Energy release temporal model for crib fire.

RESULTS

Numerical Sensitivity Study - This simulation of the wood crib fire was calculated using 24052 finite volume cells. Cell size varied from very small in regions near the fire to very large in the far reaches of the hold. Simulations with twice the number of cells produced little change in the solution convergence. Different size time steps were used for different time segments during the burn. Smaller time steps were used when calculating through large transients in the fire's thermal output and larger time steps during periods of constant thermal output. Table 1 lists the time steps. The calculation of a solution from 0 to 1500 seconds took about 80 hours to compute on an HP755. To evaluate the sensitivity of the simulation to the size of time step, a solution was computed with time steps that were half as large in each time interval as those shown in Table 1.

Table 1.Time steps used.

Time from start of fire (sec)	0-60	60-300	300-330	330-1200	1200-1500
Computational time step (sec)	1.0	5.0	1.0	5.0	1.0

A comparison of the surface temperatures on the cask at the 90 degree position, which looks directly at the burning wood crib, showed essentially no differences in results between using the two time step regimes. A more sensitive comparison was made with the

air temperatures at three heights on a pole located in the hold about 6 m from the fire. Little difference was noted at the lowest position, 0.91 m above the deck, but differences up to 5 K were recorded near the top of the pole, 2.13 m above the deck. Based on these results, it was decided that the times steps in Table 1 resulted in sufficient accuracy for the current study.

Calorimeter and Hold Temperatures - The top of the calorimeter was defined as the 0 degree location, while the 90 degree location pointed in the negative X-direction toward the fire. Temperatures were calculated for the center of each finite volume, but because of the choice in model gridding, the angular locations of these centers did not align with the thermocouple locations. Hence, in viewing results, the measured values at a given angular location had to be compared with the nearest calculated values. Only a few of these comparisons are shown here. The experimental temperatures and heating rates are presented in Koski et al., March 1997. Figure 5 is a comparison plot of measured and calculated temperatures at the 90 degree location on the calorimeter (cask). Calculated results for both transparent (no smoke) and absorbing (smoky) gas are shown with the measured values. The measured data were shifted by 390 seconds in each plot to synchronize the initial measured temperature increase with the calculated value. All of the surface temperatures shown were obtained by processing the measured and calculated temperature data through the SODDIT inverse heat transfer code (see Blackwell et al., 1987). This procedure produced more accurate estimates of temperatures at the surface of the calorimeter. A complete set of comparison plots of the measured and calculated thermal quantities is presented in Koski et al. September 1997.

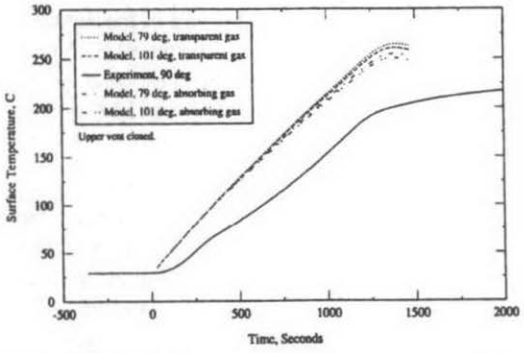

Figure 5. Calorimeter surface temperature at the 90 degree location.

In Figure 5, it can be seen that the absorbing gas calculations result in lower surface temperature predictions than do those for the transparent gas. This trend is true for all of the surface temperature comparisons. At 90 degrees, the calculated temperature increases are greater than the measured. This relationship between calculated and measured temperatures varies with location. At 60 and 270 degrees, the calculated values agreed well with the measured. The angular distributions of temperature and heating rate around the calorimeter

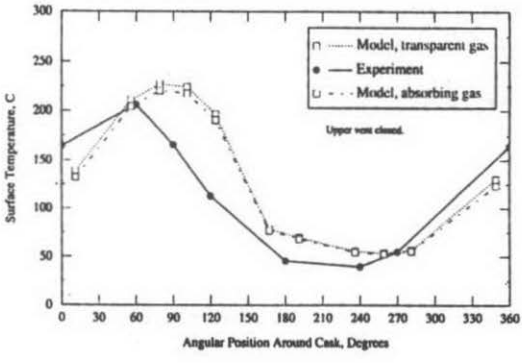

Figure 6. Surface temperatures around cask at 18 minutes.

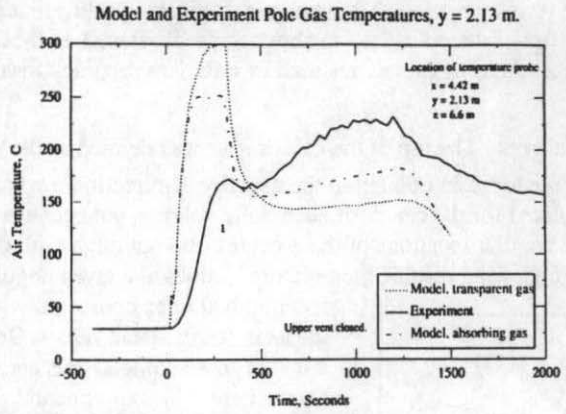

Figure 7. Gas temperature on pole, y=2.13

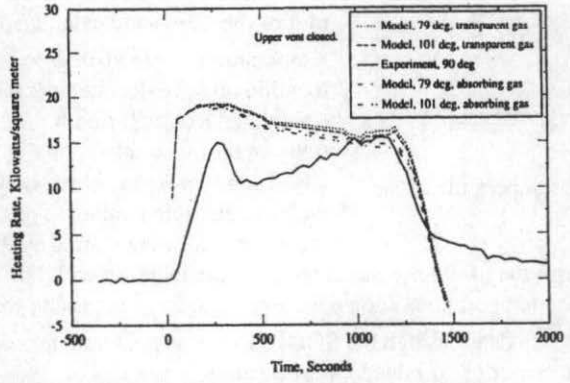

Figure 8. Heating rates on calorimeter near the 90 degree location.

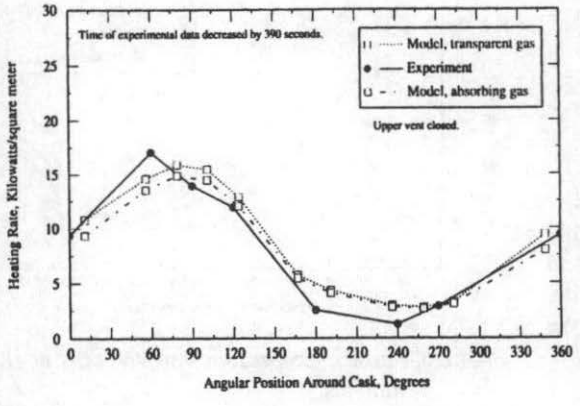

Figure 9. Heating rates around calorimeter at 18 minutes.

were examined 18 minutes after fire ignition. Figure 6 is a plot of these surface temperature distribution around the calorimeter. The measured temperatures are significantly less than the calculated temperatures mainly between 90 and 120 degrees. This disparity may be a result of the fact that the burning part of the actual wood crib started 0.36 m above the deck, whereas the model crib reached to the deck.

Figure 7 compares air temperatures about 6 m from the fire toward the starboard hull and 2.13 m above the deck. In this case the absorbing gas solution predicts air temperatures greater than the transparent gas solution and is in better agreement with the measured values. The initial overshoot in the calculated temperatures could be reduced by assigning more of the heptane energy release to the crib, which is probably what really occurred.

Calorimeter Heat Fluxes - Figure 8 is a comparison plot of the heating rates at the 90 degree location, derived from processing the calculated and measured temperature histories through the SODDIT code. On average, the calculated heating rates compare reasonably with the measured values for all locations. Again, improved modeling of the heptane energy release would probably give better agreement at the early times.

The heating rates distributed around the calorimeter at 18 minutes are shown in Figure 9. They compare very well with the measured values.

CONCLUSIONS

• Comparisons of temperatures and heating rates show that useful results can be obtained with fairly rudimentary models of the fire.

•This computational model could be used to estimate heat flux to a cask during a hold fire involving other cargo.

• More comprehensive fire models should yield better agreements with experiments

REFERENCES

Blackwell, B. F., Douglass, R. W., and Wolf, H., *A User's Manual For The Sandia One-Dimensional Direct And Inverse Thermal (SODDIT) Code,* Sandia National Laboratories Report, SAND85-2478, May 1987.

Guilbert, P. W., *Comparison of Monte Carlo and Discrete Transfer Methods for Modelling Thermal Radiation,* United Kingdom Atomic Energy Research Establishment Report AERE-R 13423, 1989.

Handbook of Geophysics and Space Environment, USAF Geophysics Laboratory, 1985.

Koski, J. A., Bobbe, J. G., Arviso, M., Wix, S. D., Beene, Jr., D. E., Byrd, R., and Graupmann, J., *Experimental Determination of the Shipboard Fire Environment for Simulated Radioactive Material Packages,* Sandia National Laboratories Report, SAND97-0506, March 1997.

Koski, J. A., Wix, S. D., and Cole, J. K., *Calculation of Shipboard Fire Conditions for Radioactive Materials Packages with the Methods of Computational Fluid Dynamics,* Sandia National Laboratories Report SAND97-2182, September 1997.